 https://doi.org/10.3311/PPme.43420

Periodica Polytechnica Mechanical Engineering, 70(1), pp. 82–88, 2026

Full Constraints Shear Testing Technique on Coarse Grained Material

Benedek Sziklai[1*], Máté Sepsi[1], Valéria Mertinger[1]

[1] Institute of Physical Metallurgy, Metalforming and Nanotechnology, Faculty of Materials and Chemical Engineering, University of Miskolc, Miskolc-Egyetemváros, H-3515 Miskolc, Hungary
[*] Corresponding author, e-mail: benedek.sziklai@uni-miskolc.hu

Received: 24 January 2026, Accepted: 11 March 2026, Published online: 17 March 2026

Abstract

With severe plastic deformation (SPD), ultra-fine grained (UFG) and nanograined materials can be produced. These materials have an exceptionally high yield stress and low strain hardening compared to coarse grained (CG) materials produced by conventional forming techniques. However, with most SPD techniques, only small-sized specimens can be made, which can be insufficient for conventional material testing. A new full constraints shear technique was proposed in a previous paper, where it was tested on UFG material and validated using finite element simulations, analytical, and numerical methods. In this paper, the testing technique was further tested on both UFG and CG materials. The chosen forming methods were the friction assisted lateral extrusion process (FALEP) and cold rolling.

Keywords

shear testing, SPD

1 Introduction

Severe plastic deformation techniques are powerful tools for producing ultrafine- or nanograined microstructures, leading to significant improvements in a wide range of material properties. However, most SPD methods remain limited to laboratory-scale applications and are difficult to upscale for large-scale industrial use. Additional drawbacks include reduced ductility and high stored energy introduced during processing, which markedly increases the driving force for recrystallisation compared to conventionally processed materials. Despite these limitations, SPD- processed materials exhibit numerous advantages, such as extremely high strength, superplasticity [1], enhanced functional properties including hydrogen storage and photocatalytic activity [2, 3], improved superconducting and thermoelectric performance [4, 5], and increased resistance to radiation, corrosion, and fatigue, as well as improved biocompatibility [6–10].

The mechanical characterization of SPD-processed materials is challenging due to their small sample sizes, limited ductility, and reduced work-hardening capacity, which restricts the applicability of conventional tensile testing. Shear testing offers a suitable alternative, as it enables large plastic deformation at lower applied loads and can be adapted to small specimen geometries. Accordingly, a novel shear testing technique was developed in a previous study [11], supported by analytical and finite element analyses, to determine the ultimate shear strength of such materials. In the present work, this approach is applied to compare two cold forming methods: conventional cold rolling and a newly developed SPD technique referred to as Friction Assisted Lateral Extrusion Process (FALEP) [12]. The sheared surfaces were also examined using Thermo Scientific Helios G4 Focused Ion Beam Scanning Electron Microscope (SEM).

2 Experimental

The testing device was introduced in more detail in the previously mentioned paper [11]. The shearing tool is composed of two symmetrical components, each consisting of five individual pieces. The exploded and assembly views of the entire testing device are shown in Fig. 1. The frame, sample holder and adjustable support pieces are made of 42CrMo4 steel, while the two shearing inserts are made of R3 high-strength steel. The assembled tool was placed between the pressure jaws of the Instron 100 kN universal material testing machine. We select the compression test mode, in which the upper tool of the tensile testing machine moves downwards until the two

Cite this article as: Sziklai, B., Sepsi, M., Mertinger, V. "Full Constraints Shear Testing Technique on Coarse Grained Material", Periodica Polytechnica Mechanical Engineering, 70(1), pp. 82–88, 2026. https://doi.org/10.3311/PPme.43420

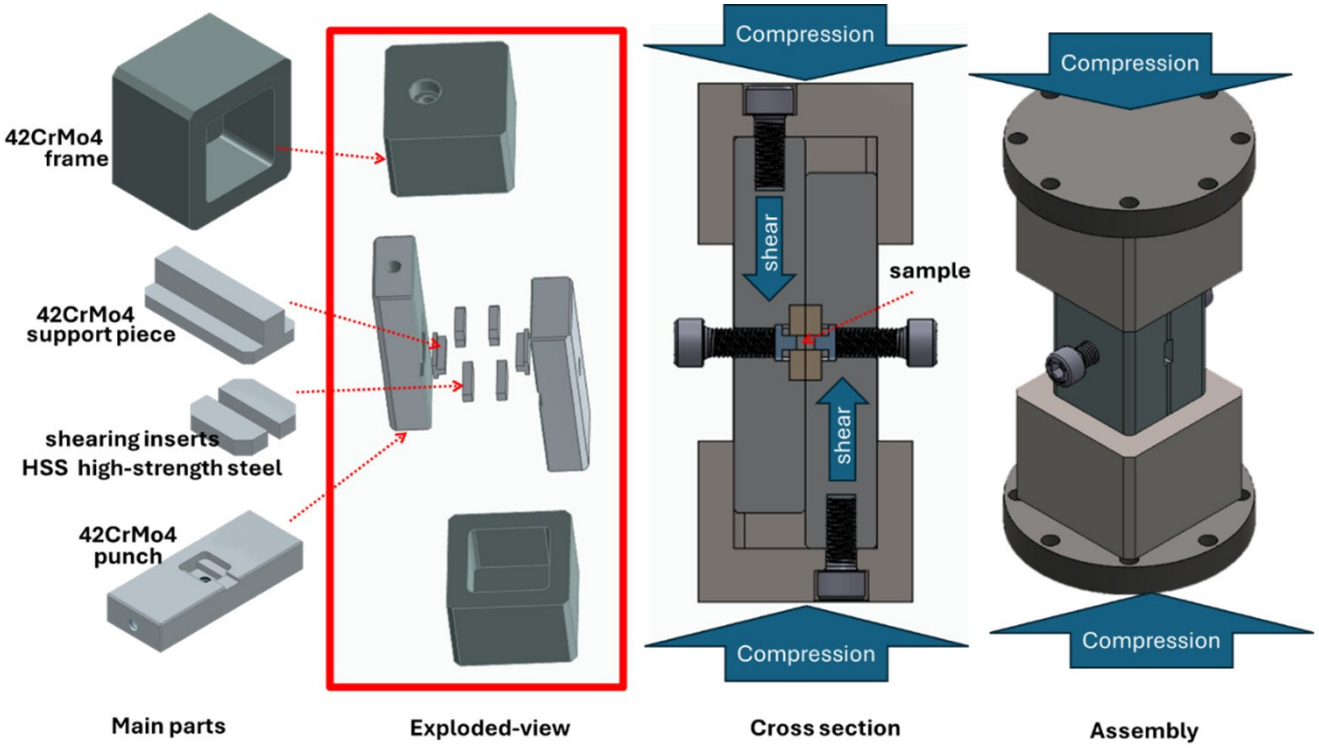

Fig. 1 Main parts, exploded, cross section and assembly views of the shear testing device

halves of the shear tool reach their end position, while the shear insert shears the test piece. When the tool reaches its end position, the upper half of the sample moves 4 mm in the direction of the pressure, while the other half remains in place, thus achieving the shear effect. The process can be stopped during operation, allowing the displacement value to vary between 0 and 4 mm. During the test, a forming speed of 5 mm/min was used, with control based on the crosshead movement, and the shear stress (τ) can be calculated by Eq. (1):

$$\tau = 1.025 \times F/(h \times w). \tag{1}$$

Where h and w are the initial height and width of the sample in the shearing zone.

Shear testing was conducted on previously deformed bulk Al 1050 specimens in two ways: an 80% reduction was applied using cold rolling and the FALEP process. In both cases, the initial thickness was 20 mm, and the final thickness was 4 mm. However, the equivalent strain (ε) of the two methods was different. For cold rolling, ε = 1.85, and for the FALEP procedure, ε = 3 was achieved. The equivalent strain for cold rolling Eq. (2) and for FALEP Eq. (3) can be defined as [12]:

$$\varepsilon_{\text{cold rolling}} = \left(\frac{2}{\sqrt{3}}\right) \times \ln\left(\frac{h_0}{h}\right) \tag{2}$$

$$\varepsilon_{\text{FALEP}} = \frac{\left(\frac{p}{c} + \frac{c}{p}\right)}{\sqrt{3}}. \tag{3}$$

Where the h_0 and p are the initial and h and c are the final thickness of the sample during rolling and FALEP deformation, respectively. Fig. 2 shows the sheets after rolling and FALEP deformation. From both sheets, 4 samples were cut out with dimensions of 4 × 4 × 20 mm. The cold rolled specimens will be referred to as R1, R2, R3, and R4, and the FALEP ones will be referred to as F1, F2, F3, and F4. The cold rolled samples grain size were above 10 µm while the FALEP processed samples were below 2 µm. These specimens were submitted to a shear test.

Before the test, the device's rigidity was characterized with a sample cut from the same material as the shearing inserts (R3 high-strength steel) with a 4 × 4 × 20 mm geometry. We conducted the investigation as follows:

1. lowered the clamp of the tensile testing machine onto the shear tool and then reset this position to zero,
2. applied a load of 50 kN to the system, measured the displacement of the crosshead, and then unloaded the system,
3. repeated this process a total of three times. These force/displacement curves are shown in Fig. 3.

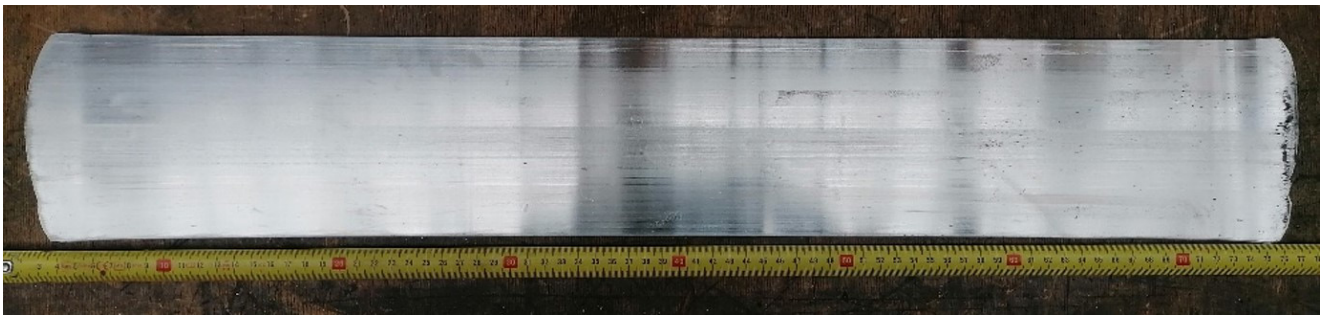

(a)

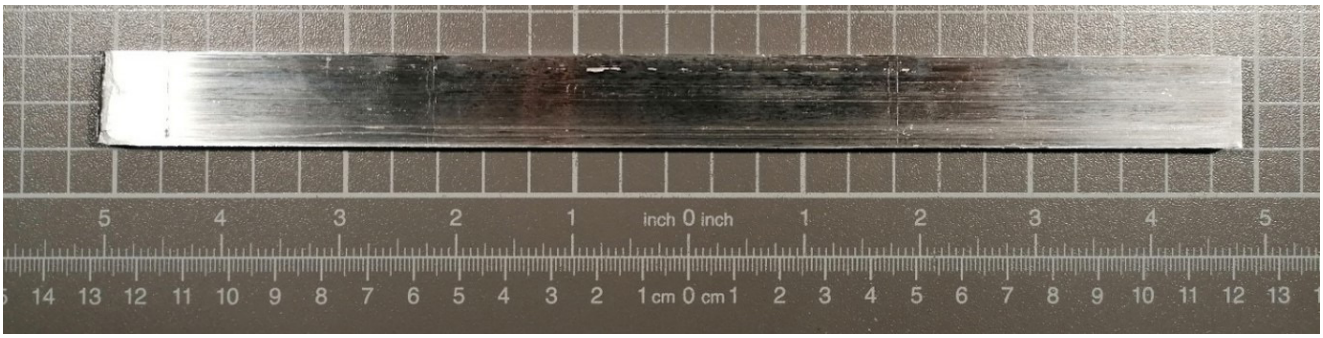

(b)

Fig. 2 The Al1050 sheets (a) after cold rolling and (b) after FALEP procedure

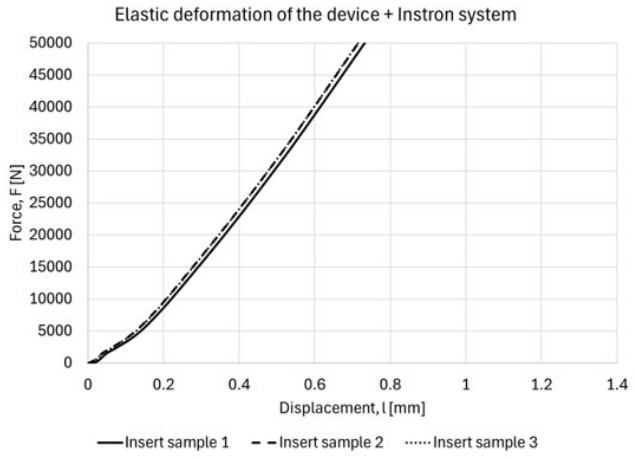

Fig. 3 The elastic deformation of the shear testing device and the Instron system

The curves clearly show that after the second load, the tool assembly moves together and behaves linearly above 2000 N. The measured results must be corrected with the results obtained in this way, which we did as follows. The data series obtained during the third load was fitted with a fifth-degree polynomial. From the force values recorded during the measurement of the test specimen, we calculated the displacement value using the polynomial. We then subtracted this value from the displacements measured by the machine, thereby obtaining the corrected displacement values for the sample.

Another result of the test is that, to obtain accurate measurements, it is advisable to preload the tool along with the sample with a value of approximately 2 kN, which corresponds to the initial value of the linear section shown in the curve. After applying the preload, the load was then removed, and the tests were subsequently started from zero load.

3 Results

The nominal stress-displacement curve shows three distinct sections, as shown in Fig. 4. The first section is the

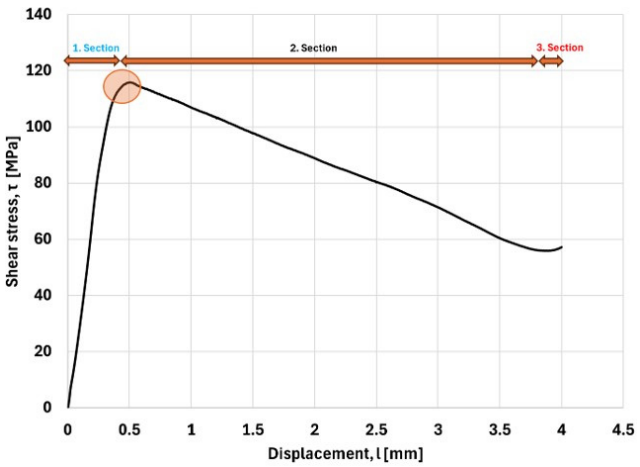

Fig. 4 Typical nominal stress displacement curve

effect of elastic deformation. This section continues until it reaches the maximum stress value, which will be determined as the shear strength of the material. From this point, the second section begins with a gradual decrease in stress levels, with varying tendencies in the two sample groups. It continues until the shearing inserts get too close to each other; this effect is evident as a sharp increase in stress by the end of the curve (third section). By the end of the experiment, the samples are deformed but remained in one piece, as shown in Fig. 5 (a), (b).

The R1–R4 cold rolled samples' curves (Fig. 6) show a good match to each other, with the difference in shear strength being only a few percent. The FALEP specimens' curves (Fig. 7) exhibit the same effect; however, the F1 samples are out of order, but not significantly, being only 10% higher than the other samples. The samples F2–F4 show a remarkable match with nearly the same strength values. The shear strength of the FALEP samples is approximately 110 MPa, while the cold-rolled samples' strength reaches only around 87 MPa, resulting in a 20% difference (Fig. 8).

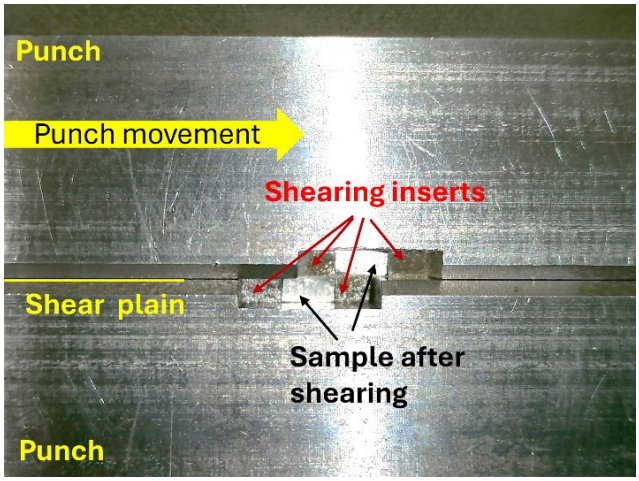

(a)

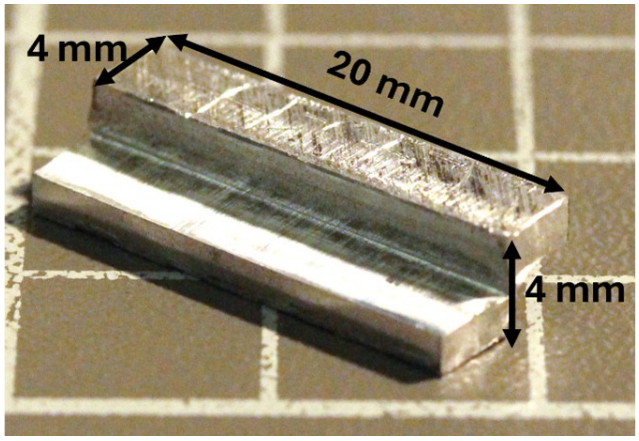

(b)

Fig. 5 (a) The tested sample in the shearing device and (b) the sample after the test

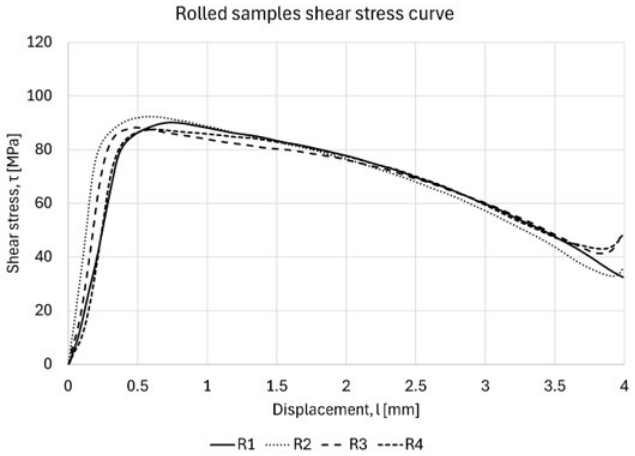

Fig. 6 Cold rolled samples' shear stress curves

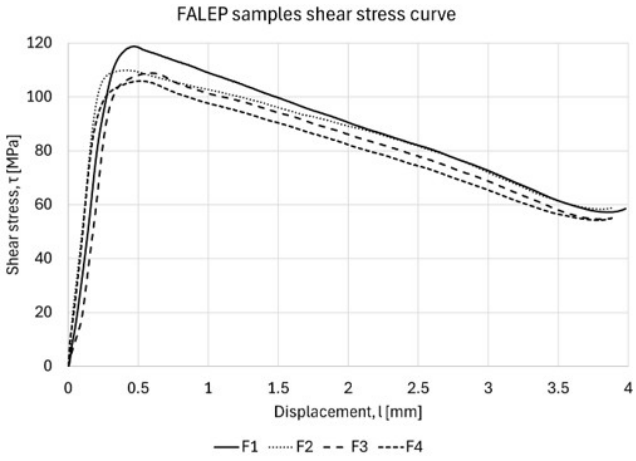

Fig. 7 FALEP samples' shear stress curves

The second section of the shear stress curves can hold more information about the forming method and the

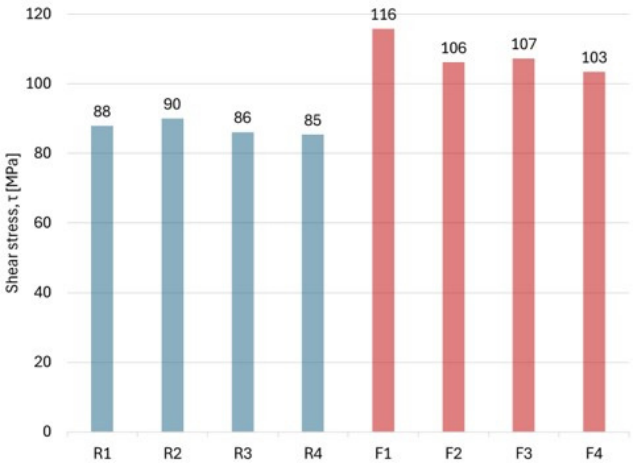

Fig. 8 The shear strength of the cold rolled and FALEP samples

shearing process as well. Therefore, they were fitted with a polynomial function. The results can be seen in Table 1. For the cold rolled samples, the functions needed to be at least a second-degree polynomial to achieve an average R^2 of 0.99. For the FALEP samples, a linear fit was sufficient to produce the same R^2 values. The use of a polynomial fitting curve indicates that the cold-rolled samples exhibited more pronounced strain hardening during the shearing process; therefore, the material did not approach its maximum hardness during rolling to the same extent as during the FALEP process.

Table 1 The fitting of the second part of the shear stress curves

Sample No.	R^2	Function
R1	0.9991	$y = -3.4878x^2 - 1.4665x + 91.729$
R2	0.9991	$y = -3.4878x^2 - 1.4665x + 91.729$
R3	0.9975	$y = -4.0814x^2 + 2.8634x + 86.808$
R4	0.9994	$y = -4.7027x^2 + 6.0081x + 82.749$
F1	0.9991	$y = -18.148x + 125.19$
F2	0.9886	$y = -15.201x + 116.51$
F3	0.996	$y = -16.485x + 116.66$
F4	0.9985	$y = -16.085x + 112.5$

After the shearing experiments, the samples' surfaces were further investigated with Scanning Electron Microscopy (SEM). Both types of samples show the same effect on the shearing surfaces (Figs. 9 and 10). At the start of shearing, the surface is smooth for around 200–250 µm in depth (Fig. 9 (c), Fig. 10 (c)). This correlates well with the first section of the shear stress curves, therefore indicating an elastic deformation. From the end of this surface, a new topology begins with long, line-like cavities that form from smaller, broken-off debris, flakes, or fragments. This "debris" is much harder and can therefore penetrate the material (Fig. 9 (b), Fig. 10 (b)). At the end of shearing the "debris" can be seen accumulating (Fig. 9 (a), Fig. 10 (a)).

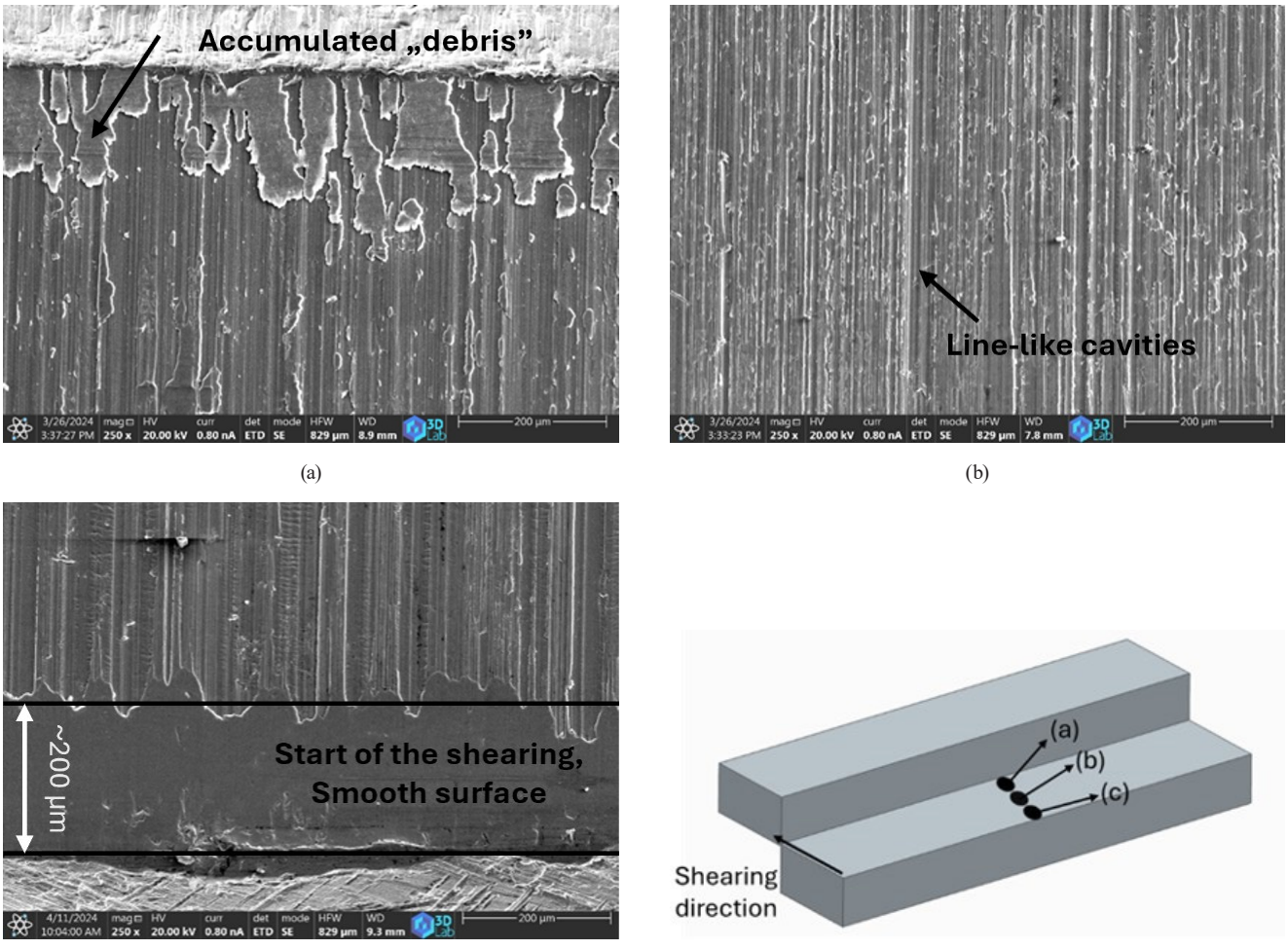

(a) (b) (c) (d)

Fig. 9 Sheared rolled samples' SEM images: (a) end of the sheared surface, (b) middle of the sheared surface, (c) the beginning of the sheared surface, (d) illustration of the sheared sample and the location of the SEM images

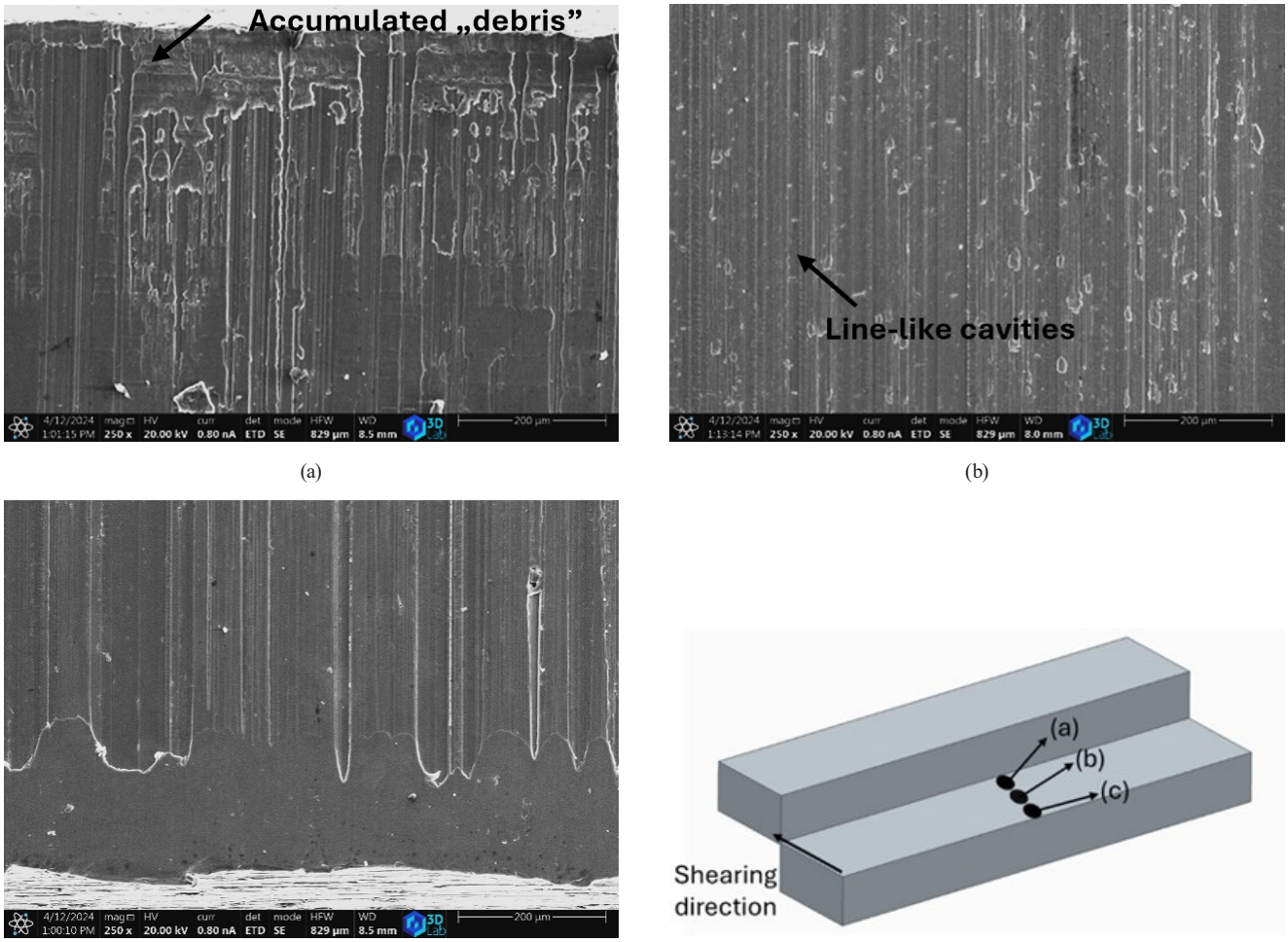

Fig. 10 Sheared FALEP samples' SEM images: (a) end of the sheared surface, (b) middle of the sheared surface, (c) the beginning of the sheared surface, (d) illustration of the sheared sample and the location of the SEM images

4 Conclusion

In this paper, the previously presented full constraints shear testing technique was used on cold rolled and FALEP produced bulk samples to determine the shear strength. During the shear testing, a 2 kN preload was applied. The resulting nominal stress displacement curves were further examined and found to have three distinct sections during shear testing. It should also be noted that the resulting shear strength showed similarities with a 10% margin of error. From the two kinds of samples, we determined that the shear strength of the FALEP samples was 20% greater than the cold-rolled ones.

Furthermore, since the nature of the fitted functions on second section of the shear stress curves differed between the two cases, the results suggest that the strain hardening behavior of the two materials during shearing is also distinct. This raises the possibility that the full constraints shear testing technique may be capable of characterizing work hardening behavior; however, a new tool design and further developments would be required to fully exploit this potential.

With these results, we were able to validate the full constraints shear testing technique convincingly on a coarse-grained material. We demonstrated that the testing technique, initially developed for characterizing composite structures and UFG bulk materials, is also suitable for CG bulk materials. We successfully applied it to characterize the hardening process of Al1050 alloy formed by different procedures. Further advantage of this method is the small sample size required.

Acknowledgements

This work was supported by the National Research, Development and Innovation Office, Hungary, under the number K143800 "New avenues of production of bulk and composite nanostructured metals; experiments,

characterization, modelling" project. The contribution of Mate Sepsi was supported by EKÖP-25-4-II/34, and Benedek Sziklai's contribution was supported by EKÖP-25-1-I/12, both of which were funded by the University Research Scholarship Program of the Ministry for Culture and Innovation, supported by the National Research, Development and Innovation Fund.

References

[1] Chinh, N. Q., Murashkin, M. Y., Bobruk, E. V., Lábár, J. L., Gubicza, J., Kovács, Z., Ahmed, A. Q., Maier-Kiener, V., Valiev, R. Z. "Ultralow-Temperature Superplasticity and Its Novel Mechanism in Ultrafine-Grained Al Alloys", Materials Research Letters, 9(11), pp. 475–482, 2021. https://doi.org/10.1080/21663831.2021.1976293

[2] Edalati, K., Bachmaier, A., Beloshenko, V. A., Beygelzimer, Y., Blank, V. D., …, Zhu, X. "Nanomaterials by Severe Plastic Deformation: Review of Historical Developments and Recent Advances", Materials Research Letters, 10(4), pp. 163–256, 2022. https://doi.org/10.1080/21663831.2022.2029779

[3] Edalati, K., Akiba, E., Horita, Z. "High-Pressure Torsion for New Hydrogen Storage Materials", Science and Technology of Advanced Materials, 19(1), pp. 185–193, 2018. https://doi.org/10.1080/14686996.2018.1435131

[4] Beloshenko, V. A., Konstantinova, T. E., Matrosov, N. I., Spuskanyuk, V. Z., Chishko, V. V., Gajda, D., Zaleski, A. J., Dyakonov, V. P., Puźniak, R., Szymczak, H. "Equal-Channel Multi-Angle Pressing Effect on the Properties of NbTi Alloy", Journal of Superconductivity and Novel Magnetism, 22(5), pp. 505–510, 2009. https://doi.org/10.1007/s10948-009-0448-y

[5] Rogl, G., Zehetbauer, M. J., Rogl, P. F. "The Effect of Severe Plastic Deformation on Thermoelectric Performance of Skutterudites, Half-Heuslers and Bi-Tellurides", Materials Transactions, 60(10), pp. 2071–2085, 2019. https://doi.org/10.2320/matertrans.MF201941

[6] Sun, C., Zheng, S., Wei, C. C., Wu, Y., Shao, L., Yang, Y., Hartwig, K. T., Maloy, S. A., Zinkle, S. J., Allen, T. R., Wang, H., Zhang, X. "Superior Radiation-Resistant Nanoengineered Austenitic 304L Stainless Steel for Applications in Extreme Radiation Environments", Scientific Reports, 5(1), 7801, 2015. https://doi.org/10.1038/srep07801

[7] Balyanov, A., Kutnyakova, J., Amirkhanova, N. A., Stolyarov, V. V., Valiev, R.Z., …, Zhu, Y. T. "Corrosion Resistance of Ultra Fine-Grained Ti", Scripta Materiala, 51(3), pp. 225–229, 2004. https://doi.org/10.1016/j.scriptamat.2004.04.011

[8] Zeiger, W., Schneider, M., Scharnweber, D., Worch, H. "Corrosion Behaviour of a Nanocrystalline FeA18 Alloy", Nanostructured Materials, 6(5–8), pp. 1013–1016, 1995. https://doi.org/10.1016/0965-9773(95)00234-0

[9] Höppel, H. W., Kautz, M., Xu, C., Murashkin, M., Langdon, T. G., Valiev, R. Z., Mughrabi, H. "An Overview: Fatigue Behaviour of Ultrafine-Grained Metals and Alloys", International Journal of Fatigue, 28(9), pp. 1001–1010, 2006. https://doi.org/10.1016/j.ijfatigue.2005.08.014

[10] Lowe, T. C., Reiss, R. A. "Understanding the Biological Responses of Nanostructured Metals and Surfaces", IOP Conference Series: Materials Science and Engineering, 63(1), 012172, 2014. https://doi.org/10.1088/1757-899X/63/1/012172

[11] Sepsi, M., Szűcs, M., Sziklai, B., Toth, L. S., Mertinger, V. "Shear Strength Measurement of Nanostructured Bulk Metals, or Interfaces, in Small Size Metal Specimen: Equipment, Testing, and Theoretical Analysis", Journal of Materials Research and Technology, 36, pp. 8517–8526, 2025. https://doi.org/10.1016/j.jmrt.2025.05.053

[12] Tóth, L. S., Sepsi, M., Szűcs, M., Kumaran, S. N., Lowe, T. C. "The Mechanics of the Friction-Assisted Lateral Extrusion Process", Journal of Materials Science, 59(14), pp. 6059–6074, 2024. https://doi.org/10.1007/s10853-023-09245-1